Computer Aided Geometric Design 73 (2019) 16–34

Contents lists available at ScienceDirect

Computer Aided Geometric Design

www.elsevier.com/locate/cagd

Deformation of spatial septic Pythagorean hodograph curves using Gauss–Legendre polygon ☆

Soo Hyun Kim, Hwan Pyo Moon *

Department of Mathematics, Dongguk University-Seoul, Seoul, 04620, Republic of Korea

ARTICLE INFO

Article history:
Received 1 October 2018
Received in revised form 7 June 2019
Accepted 8 June 2019
Available online 19 June 2019

Keywords:
Spatial Pythagorean hodograph curve
Gauss–Legendre quadrature
Rectifying control polygon
Deformation of PH curve
Quaternion representation

ABSTRACT

The notion of the rectifying control polygon of planar Pythagorean hodograph (PH) curve is extended to the spatial PH curves. We construct the Gauss–Legendre polygon by applying the Gauss–Legendre quadrature to the Pythagorean hodograph. Since the parametric speed of a PH curve is a polynomial, the Gauss–Legendre polygon with enough edges has the rectifying property, that is, the length of the polygon is the same as the length of the spatial PH curve. We also present the method to compute septic PH curves with the given Gauss–Legendre polygon. This method can be used to develop the deformation algorithm for the spatial septic PH curves.

1. Introduction

Pythagorean hodograph (PH) curves are polynomial parametric curves characterized by the property that their speed functions are also polynomials. One of the immediate advantage of PH property is the exact computation of the arc length without numerical approximation. The PH condition also induces many useful properties of curves. For example, planar PH curves have rational offsets and spatial PH curves allow rational frames. After the first introduction of planar (Farouki and Sakkalis, 1990) and spatial (Farouki and Sakkalis, 1994) PH curves, there have been a lot of researches on the construction methods for PH curves under various conditions (Farouki and Neff, 1995; Farouki and Sakkalis, 1994, 2007; Jüttler, 2001). A typical formulation of PH curve construction is the Hermite interpolation problem with various degrees of continuity at the boundary.

The algebraic structure of Pythagorean hodograph is identified as a sort of square map in the corresponding algebraic system. The planar Pythagorean hodograph is the square of a complex-valued polynomial (Farouki, 1994), and the spatial Pythagorean hodograph can be expressed as a product of a quaternion polynomial and its conjugate. These algebraic structures can be unified in the context of Clifford algebra (Choi et al., 2002). Because of the square map in the PH condition, the Hermite interpolation problems are expressed as systems of quadratic equations, so the solution might not be unique. The Hermite interpolation problems for planar PH curves usually have multiple solutions, and several selection schemes of the best solution have been reported (Choi et al., 2008; Choi and Kwon, 2008; Farouki and Neff, 1995; Moon et al., 2001). On the other hand, the Hermite interpolation problems for spatial PH curves have infinitely many solutions (Farouki et al., 2002, 2008; Kwon, 2010), which also require the selection schemes for the optimal solution.

☆ Editor: Lucia Romani.

* Corresponding author.
E-mail addresses: sookim@dongguk.edu (S.H. Kim), hpmoon@dongguk.edu (H.P. Moon).

https://doi.org/10.1016/j.cagd.2019.06.004
0167-8396/

No matter what kind of construction scheme is used, the PH curve is a polynomial curve, which can be naturally expressed as a Bézier curve. A polynomial curve can be easily controlled by its Bézier polygon. One can modify the shape of the polynomial curve for the design purpose by moving its Bézier control points. However the Bézier polygon cannot be used as the control polygon of the PH curve since an arbitrary movement of the Bézier control polygon makes the curve lose the PH property. This observation motivates the necessity of the control polygon that has the same degrees of freedom as the PH curve. The rectifying control polygon (Kim and Moon, 2017) was devised for this purpose.

The rectifying control polygon of a planar PH curve has the same degrees of freedom and the same end points as the PH curve. In addition to those, it also has the rectifying property, which means the length of the polygon is the same as the arc length of the PH curve. It is notable that a few results on the PH curve construction under the arc length constraint (Farouki, 2016; Huard et al., 2014) were reported recently. The rectifying property can be achieved by employing the Gauss–Legendre quadrature, which computes the exact integral of a polynomial function.

The goal of the present study is to generalize the concept of the rectifying control polygon from planar to spatial PH curves. For a given spatial PH curve, we construct a polygon by connecting line edges obtained by evaluating the hodograph at the Gauss–Legendre nodes. The polygons constructed by this process are called as Gauss–Legendre polygons. We will investigate the rectifying property of the Gauss–Legendre polygons.

To control the shape of a PH curve using the Gauss–Legendre polygon with the same degrees of freedom, we need to restrict the degree of the PH curve. A spatial PH curve of degree $2n+1$ has $4n+6$ degrees of freedom. Whereas the polygon of m edges has $3(m+1)$ degrees of freedom. So the first nontrivial cases are the septic PH curves with the Gauss–Legendre polygon with 5 edges. We present an algorithm to compute the septic PH curve from a given Gauss–Legendre polygon of 5 edges. The number of solutions to this problem depends on the input Gauss–Legendre polygon. We will utilize this algorithm to develop the deformation method of septic PH curves. Starting from the original septic PH curve and its Gauss–Legendre polygon, we apply slight modification to the polygon. The corresponding septic PH curves can be computed by solving a system of trigonometric equations. We can solve the nonlinear system by Newton–Raphson method with the initial approximation from the original PH curve. For a large modification of the Gauss–Legendre polygon, we subdivide the change into small steps and apply the previous step repeatedly. Using this homotopy method, we are able to deform the septic PH curve according to our design purpose.

The remainder of the paper is organized as follows. In section 2, we review the quaternion representation of spatial PH curves and fix the notations. Section 3 is devoted to the construction of the rectifying polygon of spatial PH curves using Gauss–Legendre quadrature. In Section 4, we solve the inverse problem of Section 3. We present the method to find septic PH curves with given Gauss–Legendre polygon. We investigate the solvability conditions for this problem in Section 5. By repeatedly solving this problem for the moving Gauss–Legendre polygon, we develop the algorithm for the deformation of spatial septic PH curves in Section 6. The closing remark and future work will be given in Section 7.

2. Quaternion representation of Pythagorean hodograph

A spatial polynomial curve $\mathbf{p}(t) = \big(x(t),\ y(t),\ z(t)\big)$ is called a *spatial Pythagorean hodograph (PH)* curve if and only if its derivative $\mathbf{p}'(t) = \big(x'(t),\ y'(t),\ z'(t)\big)$ satisfies the Pythagorean condition

$$x'(t)^2 + y'(t)^2 + z'(t)^2 = \sigma(t)^2 \tag{1}$$

for some polynomial $\sigma(t)$. An equivalent condition to (1) is the existence of four polynomials $u(t)$, $v(t)$, $p(t)$ and $q(t)$ that satisfy

$$\begin{aligned} x'(t) &= u(t)^2 + v(t)^2 - p(t)^2 - q(t)^2, \\ y'(t) &= 2u(t)q(t) + 2v(t)p(t), \\ z'(t) &= 2v(t)q(t) - 2u(t)p(t). \end{aligned} \tag{2}$$

These algebraic relations can be expressed in a compact form by using quaternions. The space of quaternions, denoted by $\mathbb{H}$, is a 4 dimensional linear space with basis 1, $\mathbf{i}$, $\mathbf{j}$, $\mathbf{k}$. This space has the non-commutative algebraic structure with the multiplication defined by the relations

$$\mathbf{i}^2 = \mathbf{j}^2 = \mathbf{k}^2 = \mathbf{ijk} = -1.$$

These relations induce additional multiplicative rules such as

$$\mathbf{ij} = -\mathbf{ji} = \mathbf{k}, \quad \mathbf{jk} = -\mathbf{kj} = \mathbf{i}, \quad \mathbf{ki} = -\mathbf{ik} = \mathbf{j}.$$

When we denote a quaternion $\mathcal{A}$ as

$$\mathcal{A} = a + x\,\mathbf{i} + y\,\mathbf{j} + z\,\mathbf{k},$$

a is called as the scalar part of $\mathcal{A}$, and $x\,\mathbf{i} + y\,\mathbf{j} + z\,\mathbf{k}$ is called as the vector part of $\mathcal{A}$. A quaternion with the vanishing scalar part is called as a pure quaternion, which can be naturally identified to a vector in $\mathbb{R}^3$. The set of all pure quaternions will

be denoted by $\mathbb{H}^\times$, which is isomorphic to $\mathbb{R}^3$. The conjugate of $\mathcal{A}$ is defined by $\mathcal{A}^* = a - x\mathbf{i} - y\mathbf{j} - z\mathbf{k}$, and the norm of $\mathcal{A}$ is defined by

$$|\mathcal{A}| = \sqrt{\mathcal{A}\mathcal{A}^*} = \sqrt{a^2 + x^2 + y^2 + z^2}.$$

In the context of algebra, the space of quaternions is a division algebra (Hungerford, 1974) with the multiplicative inverse

$$\mathcal{A}^{-1} = \frac{\mathcal{A}^*}{|\mathcal{A}|^2} = \frac{1}{a^2 + x^2 + y^2 + z^2}(a - x\mathbf{i} - y\mathbf{j} - z\mathbf{k})$$

for all nonzero quaternions $\mathcal{A} = a + x\mathbf{i} + y\mathbf{j} + z\mathbf{k}$. A quaternion $\mathcal{A}$ with $|\mathcal{A}| = 1$ is then called a unit quaternion. Note that a pure unit quaternion corresponds to a unit vector in $\mathbb{R}^3$.

Using the identification between $\mathbb{R}^3$ and the pure quaternions, a spatial curve can be expressed as a curve in the space of pure quaternions. So the spatial curve $\mathbf{p}(t) = \big(x(t),\ y(t),\ z(t)\big)$ can be written as

$$\mathbf{p}(t) = x(t)\,\mathbf{i} + y(t)\,\mathbf{j} + z(t)\,\mathbf{k}.$$

The three identities in Equation (2) can then be expressed as

$$\mathbf{p}'(t) = \mathcal{A}(t)\,\mathbf{i}\,\mathcal{A}(t)^* \tag{3}$$

where $\mathcal{A}(t)$ is the quaternion polynomial given by $\mathcal{A}(t) = u(t) + v(t)\,\mathbf{i} + p(t)\,\mathbf{j} + q(t)\,\mathbf{k}$. Note that the scalar part of the product $\mathcal{A}(t)\,\mathbf{i}\,\mathcal{A}(t)^*$ always vanishes. The speed of $\mathbf{p}(t)$, which corresponds to $\sigma(t)$ in Equation (1), can be obtained by

$$\sigma(t) = |\mathbf{p}(t)| = \left|\mathcal{A}(t)\,\mathbf{i}\,\mathcal{A}(t)^*\right| = u(t)^2 + v(t)^2 + p(t)^2 + q(t)^2.$$

We now discuss the geometric meaning of Equation (1). If $\mathcal{A}$ is a unit quaternion, then we can express $\mathcal{A}$ as

$$\mathcal{A} = \cos\frac{\theta}{2} + \sin\frac{\theta}{2}\,\mathbf{a}$$

where $\mathbf{a}$ is a unit pure quaternion and θ is a real number in the range $(-\pi, \pi]$. For a fixed pure quaternion $\mathbf{c}$, it is well known that the product $\mathcal{A}\,\mathbf{c}\,\mathcal{A}^*$ produces the pure quaternion that corresponds to the rotation of $\mathbf{c}$ through the angle θ around the axis of rotation $\mathbf{a}$. So if we express the quaternion polynomial $\mathcal{A}(t)$ as

$$\mathcal{A}(t) = |\mathcal{A}(t)|\left(\cos\frac{\theta(t)}{2} + \sin\frac{\theta(t)}{2}\,\mathbf{a}(t)\right)$$

with a pure unit quaternion $\mathbf{a}(t)$, then the spatial Pythagorean hodograph $\mathbf{p}'(t) = \mathcal{A}(t)\,\mathbf{i}\,\mathcal{A}(t)^*$ is the vector generated by applying the rotation of the angle $\theta(t)$ around the axis $\mathbf{a}(t)$ and the scaling of the magnitude $|\mathcal{A}(t)|^2$ to a fixed vector $\mathbf{i}$.

In the quaternion representation of PH curves, the symmetric expression $\mathcal{A}\,\mathbf{i}\,\mathcal{B}^* + \mathcal{B}\,\mathbf{i}\,\mathcal{A}^*$ for two quaternions $\mathcal{A}$ and $\mathcal{B}$ appears repeatedly. So the notation introduced in Šír and Jüttler (2007) simplifies the presentations quite a lot. The binary operation $\star$ on quaternions in defined by

$$\mathcal{A} \star \mathcal{B} = \frac{1}{2}\left(\mathcal{A}\,\mathbf{i}\,\mathcal{B}^* + \mathcal{B}\,\mathbf{i}\,\mathcal{A}^*\right),$$

and the corresponding n-th power is denoted by $\mathcal{A}^{n\star}$. Note that $\mathcal{A} \star \mathcal{B}$ is always a pure quaternion, which is the vector part of $\mathcal{A}\,\mathbf{i}\,\mathcal{B}^*$. The construction problem of spatial PH curves often requires the solution of quaternion equation

$$\mathcal{A}^{2\star} = \mathcal{A}\,\mathbf{i}\,\mathcal{A}^* = \mathbf{c}$$

for a pure quaternion $\mathbf{c}$. Let us denote the unit vector in the direction of $\mathbf{c}$ as $\mathbf{c}/|\mathbf{c}| = (\lambda, \mu, \nu)$. It is known (Farouki et al., 2002) that the solution to the previous equation is the one parameter family

$$\mathcal{A}(\phi) = \sqrt{\frac{1}{2}(1+\lambda)|\mathbf{c}|}\left(\mathbf{i} + \frac{\mu}{1+\lambda}\mathbf{j} + \frac{\nu}{1+\lambda}\mathbf{k}\right)\mathcal{Q}(\phi)$$

where $\mathcal{Q}(\phi) = \cos\phi + \sin\phi\,\mathbf{i}$. This solution is valid if $\mathbf{c}$ is not a negative multiple of $\mathbf{i}$. It is also written (Farouki et al., 2008; Šír and Jüttler, 2007) as

$$\mathcal{A}(\phi) = \sqrt{|\mathbf{c}|}\,\frac{\frac{\mathbf{c}}{|\mathbf{c}|} + \mathbf{i}}{\left|\frac{\mathbf{c}}{|\mathbf{c}|} + \mathbf{i}\right|}\,\mathcal{Q}(\phi).$$

Among the one parameter family of solutions, there exists a unique pure quaternion solution $\mathcal{A}(0)$. This particular solution is the vector pointing in the middle direction between $\mathbf{c}$ and $\mathbf{i}$ with the magnitude $\sqrt{|\mathbf{c}|}$. We here introduce a notation for this particular solution.

Definition 1. For a pure quaternion $\mathbf{c}$ that is not a negative multiple of $\mathbf{i}$, the $\star$-*square root* is defined by

$$\sqrt[\star]{\mathbf{c}} = \sqrt{|\mathbf{c}|}\,\frac{\frac{\mathbf{c}}{|\mathbf{c}|}+\mathbf{i}}{\left|\frac{\mathbf{c}}{|\mathbf{c}|}+\mathbf{i}\right|}.$$

It is easy to see that the $\star$-square root can also be expressed as

$$\sqrt[\star]{\mathbf{c}} = \frac{\mathbf{c}+|\mathbf{c}|\,\mathbf{i}}{\sqrt{2(|\mathbf{c}|+c_x)}}$$

where $\mathbf{c} = c_x\,\mathbf{i} + c_y\,\mathbf{j} + c_z\,\mathbf{k}$. It is also worth noting that the ambiguity of the $\star$-square root for the negative multiple of $\mathbf{i}$ is analogous to the branch cut of the complex square root along the negative real axis. When $\mathbf{c}$ is a negative multiple of $\mathbf{i}$, say $\mathbf{c} = -c\,\mathbf{i}$ for $c > 0$, the pure quaternion solutions of $\mathcal{A}^{2\star} = -c\,\mathbf{i}$ are $\sqrt{c}\,(\sin\phi\,\mathbf{j} + \cos\phi\,\mathbf{k})$. So we can extend the definition of the $\star$-square root to $\sqrt[\star]{-c\,\mathbf{i}} = \sqrt{c}\,\mathbf{k}$. Then all solutions of $\mathcal{A}^{2\star} = \mathbf{c}$ can be obtained by $\sqrt[\star]{\mathbf{c}}\,\mathcal{Q}(\phi)$.

3. Rectifying polygon of spatial PH curves

We here clarify the definition of the rectifying polygon (Kim and Moon, 2017).

Definition 2. For a given PH curve $\mathbf{p}(t)$, a polygon, denoted by $[\mathbf{p}_0 \cdots \mathbf{p}_{n+1}]$, connecting the sequence of points $\mathbf{p}_0, \cdots, \mathbf{p}_{n+1}$, is called a *rectifying polygon* (Kim and Moon, 2017) if it satisfies the following properties:

(i) the end point interpolation, that is, $\mathbf{p}(0) = \mathbf{p}_0$, $\mathbf{p}(1) = \mathbf{p}_{n+1}$,
(ii) the rectifying property, which means the length of the polygon $[\mathbf{p}_0 \cdots \mathbf{p}_{n+1}]$ is the same as the length of the PH curve $\mathbf{p}(t)$.

Moreover, a rectifying polygon $[\mathbf{p}_0 \cdots \mathbf{p}_{n+1}]$ is called a *rectifying control polygon* if it satisfies the following condition:

(iii) the polygon has the same degrees of freedom as the PH curve has.

In this section, we focus only on *rectifying polygons* of a PH curve. The conditions of a rectifying polygon can be easily achieved by many polygons even with limited number of edges. For example, suppose $\mathbf{p}(t)$ is a planar PH curve of the arc length L. One can construct a rectifying polygon $[\mathbf{p}_0\mathbf{p}_1\mathbf{p}_2]$ with only two edges by setting $\mathbf{p}_0 = \mathbf{p}(0)$, $\mathbf{p}_2 = \mathbf{p}(1)$, and choosing $\mathbf{p}_1$ as a point on the ellipse that is defined by $\mathbf{p}_0$, $\mathbf{p}_2$ as its foci and the major axis length L. However, we are interested in the rectifying polygon that has enough edges to represent the shape of the given PH curve.

For this purpose, we employ Gauss–Legendre quadrature, which approximates the integral of the function f defined on the interval $[-1, 1]$. The Legendre polynomial $P_m(t)$ on $[-1, 1]$ is defined by

$$P_m(t) = \frac{(-1)^m}{m!\,2^m}\frac{d^m}{dt^m}\left[\left(1-t^2\right)^m\right]$$

for $m = 0, 1, 2, \cdots$. Then $P_m(t)$ is the polynomial of degree m, and has m distinct real roots on $[-1, 1]$. These real roots are denoted by $\tau_{m,k}$ for $k = 0, \cdots, m-1$ in increasing order. The Gauss–Legendre quadrature of f with m node points is then defined by

$$I_m(f; [-1, 1]) = \sum_{k=0}^{m-1} \omega_{m,k}\, f(\tau_{m,k}),$$

where the weights $\omega_{m,k}$ are

$$\omega_{m,k} = \frac{-2}{(m+1)P'_m(\tau_{m,k})P_{m+1}(\tau_{m,k})}.$$

Since this formulation is for the integral over the interval $[-1, 1]$, we need to scale the nodes and the weights for the integral over the interval $[0, 1]$. The integral $\int_0^1 f(t)\,dt$ can be approximated by

$$I_m(f) = I_m(f; [0, 1]) = \sum_{k=0}^{m-1} \frac{\omega_{m,k}}{2} f\left(\frac{1+\tau_{m,k}}{2}\right).$$

One may consult (Kim and Moon, 2017) for more discussion on Gauss–Legendre quadrature and the values of $\tau_{m,k}$ and $\omega_{m,k}$ for small m's. The values of nodes $\tau_{m,k}$ and weights $\omega_{m,k}$ can be computed symbolically only for $m \le 5$. It is inevitable to employ numerical method to find the roots of Legendre polynomial for $m \ge 6$.

A notable property of Gauss–Legendre quadrature is that it gives the exact integral of the polynomials of the maximal degree with the given number of nodes. The Gauss–Legendre quadrature with m node points computes the integral of polynomials of degree up to $2m-1$ exactly. This property enables us to compute the arc length of PH curves exactly by the Gauss–Legendre quadrature with finite number of nodes, because the speed of a PH curve is a polynomial function.

We now define a polygon that mimics the shape of a given curve by using Gauss–Legendre quadrature. This definition is valid not only for PH curves but also for any regular curves.

Definition 3. Let $\mathbf{p}$ be a regular spatial curve defined on $[0,1]$. The *Gauss–Legendre polygon* of $\mathbf{p}$ with m edges is defined by

$$G_m(\mathbf{p}) = [\mathbf{p}_0 \cdots \mathbf{p}_m]$$

where

$$\mathbf{p}_0 = \mathbf{p}(0),$$
$$\mathbf{p}_{k+1} = \mathbf{p}_k + \frac{\omega_{m,k}}{2}\mathbf{p}'\left(\frac{1+\tau_{m,k}}{2}\right) \quad \text{for } k = 0, \cdots, m-1.$$

Theorem 3 in Kim and Moon (2017) states that the Gauss–Legendre polygon of a planar PH curve is the rectifying polygon if the appropriate number of nodes are used. Although the proof of this theorem can be used for spatial PH curves without alteration, we here reformulate the result in two steps. A regular curve $\mathbf{p}$ and its Gauss–Legendre polygon share the same starting point by definition. If $\mathbf{p}$ is a polynomial curve, then its Gauss–Legendre polygon has the end point interpolation property in the following context.

Theorem 4. *Let $\mathbf{p}$ be a polynomial curve of degree l defined on $[0,1]$. If $m > l/2$, then the Gauss–Legendre polygon $G_m(\mathbf{p})$ has the end point interpolation property; that is, $\mathbf{p}_m = \mathbf{p}(1)$.*

Proof. Let $\mathbf{p}(t) = \big(x(t),\, y(t),\, z(t)\big)$ and $\mathbf{p}_k = \big(x_k,\, y_k,\, z_k\big)$ for $k = 0, \cdots, m$ where $G_m(\mathbf{p}) = [\mathbf{p}_0 \cdots \mathbf{p}_m]$. Since the end point interpolation property can be verified for each coordinate separately, it suffices to show it for a particular coordinate, say x. Starting from $x_0 = x(0)$, the x-coordinates of the points of $G_m(\mathbf{p})$ satisfy

$$x_{k+1} = x_k + \frac{\omega_{m,k}}{2}x'\left(\frac{1+\tau_{m,k}}{2}\right).$$

So the x-coordinate of the final point $\mathbf{p}_m$ is

$$x_m = x_0 + \sum_{k=0}^{m-1}\frac{\omega_{m,k}}{2}x'\left(\frac{1+\tau_{m,k}}{2}\right).$$

The summation above is the Gauss–Legendre quadrature of $x'(t)$. Since $x'(t)$ is a polynomial of degree $l-1$, this quadrature provides the exact integral if $l-1 \le 2m-1$. In this case, we get

$$x_m = x_0 + \int_0^1 x'(t)\,dt = x(1). \quad \square$$

In addition to the end point interpolation property, the Gauss–Legendre polygon acquires the rectifying property if the given curve $\mathbf{p}$ is a PH curve.

Theorem 5. *Let $\mathbf{p}$ be a PH curve of degree $2n+1$ defined on $[0,1]$. If $m \ge n+1$, then the Gauss–Legendre polygon $G_m(\mathbf{p})$ is a rectifying polygon.*

Proof. If $m \ge n+1$, then $m \ge n/2$ for positive n. So $G_m(\mathbf{p})$ has the end point interpolation property by Theorem 4. We only need to show the rectifying property. The length of $G_m(\mathbf{p}) = [\mathbf{p}_0 \cdots \mathbf{p}_m]$ can be expressed as

$$\sum_{k=0}^{m-1}\left|\mathbf{p}_{k+1} - \mathbf{p}_k\right| = \sum_{k=0}^{m-1}\frac{\omega_{m,k}}{2}\left|\mathbf{p}'\left(\frac{1+\tau_{m,k}}{2}\right)\right|.$$

The summation on right hand side is the Gauss–Legendre quadrature of the speed function $\sigma(t) = |\mathbf{p}'(t)|$, which is a polynomial of degree $2n$. When $m \ge n+1$, the degree $2n$ of the speed $\sigma(t)$ is less than $2m-1$. So the Gauss–Legendre quadrature produces the exact integral of $\sigma(t)$, which is the arc length of $\mathbf{p}$. $\square$

In this article, we deal mainly with *septic* PH curves. The reason for the interest on the PH curves of this particular degree will be clear in the next section. We here present an example of the Gauss–Legendre polygon for a septic PH curve. To define a spatial septic PH curve, we begin with a cubic quaternion polynomial

$$\mathcal{A}(t) = \sum_{i=0}^{3} B_i^3(t)\mathcal{A}_i, \tag{4}$$

where $B_i^n(t) = \binom{n}{i}(1-t)^{n-i}t^i$ are the Bernstein basis polynomials. The Bézier control points of the septic PH curve $\mathbf{p}(t)$ obtained by integrating the hodograph $\mathbf{p}'(t) = \mathcal{A}(t)\,\mathbf{i}\,\mathcal{A}(t)^*$ are then given in terms of the quaternion coefficients $\mathcal{A}_0,\ \mathcal{A}_1,\ \mathcal{A}_2,\ \mathcal{A}_3$ by

$$\begin{aligned}
\mathbf{b}_1 &= \mathbf{b}_0 + \frac{1}{7}\mathcal{A}_0^{2\star},\\
\mathbf{b}_2 &= \mathbf{b}_1 + \frac{1}{7}\,\mathcal{A}_0 \star \mathcal{A}_1,\\
\mathbf{b}_3 &= \mathbf{b}_2 + \frac{1}{35}\left(2\,\mathcal{A}_0 \star \mathcal{A}_2 + 3\,\mathcal{A}_1^{2\star}\right),\\
\mathbf{b}_4 &= \mathbf{b}_3 + \frac{1}{70}\left(\mathcal{A}_0 \star \mathcal{A}_3 + 9\,\mathcal{A}_1 \star \mathcal{A}_2\right),\\
\mathbf{b}_5 &= \mathbf{b}_4 + \frac{1}{35}\left(2\,\mathcal{A}_1 \star \mathcal{A}_3 + 3\,\mathcal{A}_2^{2\star}\right),\\
\mathbf{b}_6 &= \mathbf{b}_5 + \frac{1}{7}\,\mathcal{A}_2 \star \mathcal{A}_3,\\
\mathbf{b}_7 &= \mathbf{b}_6 + \frac{1}{7}\mathcal{A}_3^{2\star},
\end{aligned} \tag{5}$$

where $\mathbf{b}_0$ is the starting point of $\mathbf{p}(t)$. In this case, the parametric speed $\sigma(t)$ is the polynomial of degree 6 whose Bernstein coefficients are

$$\begin{aligned}
\sigma_0 &= |\mathcal{A}_0|^2, \qquad \sigma_1 = |\mathcal{A}_0 \star \mathcal{A}_1|,\\
\sigma_2 &= \frac{1}{5}\left|2\,\mathcal{A}_0 \star \mathcal{A}_2 + 3\,\mathcal{A}_1^{2\star}\right|,\\
\sigma_3 &= \frac{1}{10}\left|\mathcal{A}_0 \star \mathcal{A}_3 + 9\,\mathcal{A}_1 \star \mathcal{A}_2\right|,\\
\sigma_4 &= \frac{1}{5}\left|2\,\mathcal{A}_1 \star \mathcal{A}_3 + 3\,\mathcal{A}_2^{2\star}\right|,\\
\sigma_5 &= |\mathcal{A}_2 \star \mathcal{A}_3|, \qquad \sigma_6 = |\mathcal{A}_3|^2.
\end{aligned} \tag{6}$$

We now present an illustrative example of the Gauss–Legendre polygon of a septic PH curve.

Example 6. Let $\mathbf{p}$ be the septic PH curve generated by the cubic polynomial $\mathcal{A}(t)$ with quaternion coefficients

$$\begin{aligned}
\mathcal{A}_0 &= -0.334326 + 2.187596\,\mathbf{i} + 0.068209\,\mathbf{j} + 0.393061\,\mathbf{k},\\
\mathcal{A}_1 &= 2.367021 + 0.059904\,\mathbf{i} + 0.556554\,\mathbf{j} + 0.825115\,\mathbf{k},\\
\mathcal{A}_2 &= -2.123865 - 1.208449\,\mathbf{i} - 2.986226\,\mathbf{j} - 0.027264\,\mathbf{k},\\
\mathcal{A}_3 &= 2.136875 + 0.885587\,\mathbf{i} + 0.057586\,\mathbf{j} + 0.602801\,\mathbf{k}.
\end{aligned}$$

Fig. 1 illustrates the septic PH curve as the cyan curve and the Bézier control polygon computed by Equations (5) as the green polygon. By Theorem 5, the Gauss–Legendre polygon $G_m(\mathbf{p})$ of the septic PH curve $\mathbf{p}$ has the rectifying property if the number of nodes $m \geq 4$. The computed $G_4(\mathbf{p})$ is shown as the blue polygon in Fig. 1, and its rectifying property has been confirmed numerically. The arc-length of $\mathbf{p}$ is the integral of the speed function $\sigma(t)$ that is the polynomial of degree 6 with the coefficients given in Equation (6). On the other hand, the length of $G_4(\mathbf{p})$ is the sum of the length of each edge $\overline{\mathbf{p}_k\mathbf{p}_{k+1}}$ for $k = 0, 1, 2, 3$. Both methods result in the same numerical value $L = 1.858309$. The Gauss–Legendre polygon with different number of node points can also be constructed easily. Fig. 2 illustrates the Gauss–Legendre polygon $G_m(\mathbf{p})$ together with its length for $m = 1, 2, \cdots, 6$. They have the rectifying property for $m \geq 4$.

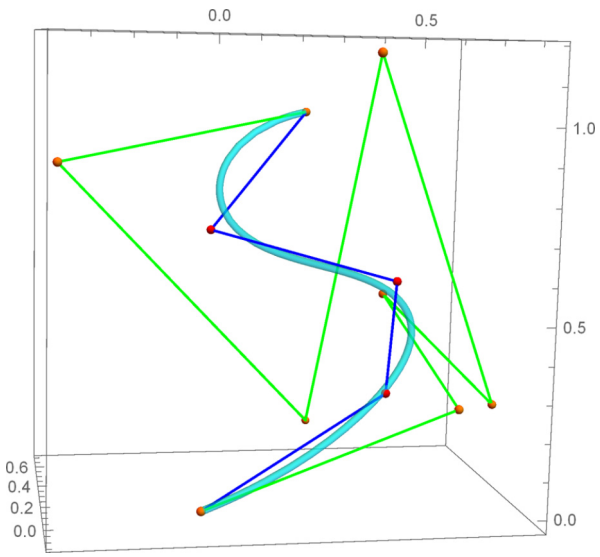

Fig. 1. A septic PH curve is shown in cyan curve together with its Bézier polygon (green) and its Gauss–Legendre polygon $G_4(\mathbf{p})$ (blue). (For interpretation of the colors in the figure(s), the reader is referred to the web version of this article.)

4. Septic PH curves of prescribed Gauss–Legendre polygon

Our goal in this article is to derive the algorithm to change the shape of a spatial septic PH curve smoothly for the user's design purpose. One cannot simply move a Bézier control point of a PH curve since it results in violating the PH condition. One possible way to deform the PH curve $\mathbf{p}$ smoothly while maintaining the PH property is changing the quaternion polynomial $\mathcal{A}(t)$ that generates the hodograph as $\mathbf{p}'(t) = \mathcal{A}(t)\,\mathbf{i}\,\mathcal{A}(t)^*$. However this approach is not intuitive since it is difficult to predict the effect of the change of $\mathcal{A}(t)$ to the shape of the PH curve. We address this problem by employing the rectifying control polygon, which has the same degrees of freedom with the given PH curve. Since a polygon $[\mathbf{p}_0 \cdots \mathbf{p}_m]$ of m edges has $3(m+1)$ degrees of freedom, this approach will be applicable to PH curves whose degrees of freedom is the integer multiple of 3. So we need to analyze the degrees of freedom of spatial PH curves.

Lemma 7. *If* $\mathbf{p}$ *is a PH curve of degree* $2n+1$*, then it has* $4n+6$ *degrees of freedom.*

Proof. A PH curve of degree $2n+1$ is generated by integrating $\mathbf{p}'(t) = \mathcal{A}(t)\,\mathbf{i}\,\mathcal{A}(t)^*$, where $\mathcal{A}(t)$ is a quaternion polynomial of degree n. Since $\mathcal{A}(t)$ has $n+1$ quaternion coefficients, its degrees of freedom is $4n+4$. But we loose 1 degree of freedom while computing the hodograph $\mathbf{p}'(t)$ since $\widetilde{\mathcal{A}}(t) = \mathcal{A}(t)\mathcal{Q}(\theta)$ produces the same hodograph, that is,

$$\widetilde{\mathcal{A}}(t)\,\mathbf{i}\,\widetilde{\mathcal{A}}(t)^* = \mathcal{A}(t)\,\mathcal{Q}(\theta)\,\mathbf{i}\,\mathcal{Q}(\theta)^*\mathcal{A}(t)^* = \mathcal{A}(t)\,\mathbf{i}\,\mathcal{A}(t)^*. \tag{7}$$

Thus the hodograph $\mathbf{p}'(t)$ has $4n+3$ degrees of freedom. Finally the PH curve gains 3 more degrees of freedom from the integral constant $\mathbf{p}(0)$. □

The first nontrivial PH curves whose degrees of freedom is a multiple of 3 arise when $n = 3$. That corresponds to the PH curve of degree 7, or the *septic* PH curve. Since the number of degrees of freedom of a septic PH curve is 18, the Gauss–Legendre polygon $G_5(\mathbf{p})$, which consists of 6 points in $\mathbb{R}^3$, becomes the rectifying control polygon. For the deformation of the septic PH curve $\mathbf{p}$, we first construct its Gauss–Legendre polygon $G_5(\mathbf{p}) = [\mathbf{p}_0 \cdots \mathbf{p}_5]$. Then we move the points of $G_5(\mathbf{p})$ to desired position, which modifies the shape of the corresponding PH curve. Thus we need the method of computing the septic PH curve from its Gauss–Legendre polygon.

From now on, we will focus only on septic PH curves and their Gauss–Legendre polygon $G_5(\mathbf{p})$. When we fix the number of nodes $m = 5$, we can simplify the notations for the Gauss–Legendre nodes $\tau_{5,k}$ and the weights $\omega_{5,k}$ to τ_k and ω_k, respectively. These values are shown in Table 1.

Our problem can then be formulated by using the Bernstein–Vandermonde matrix of cubic Bernstein basis at the nodes $(1+\tau_k)/2$ for $k = 0, \cdots, 4$, which is given by

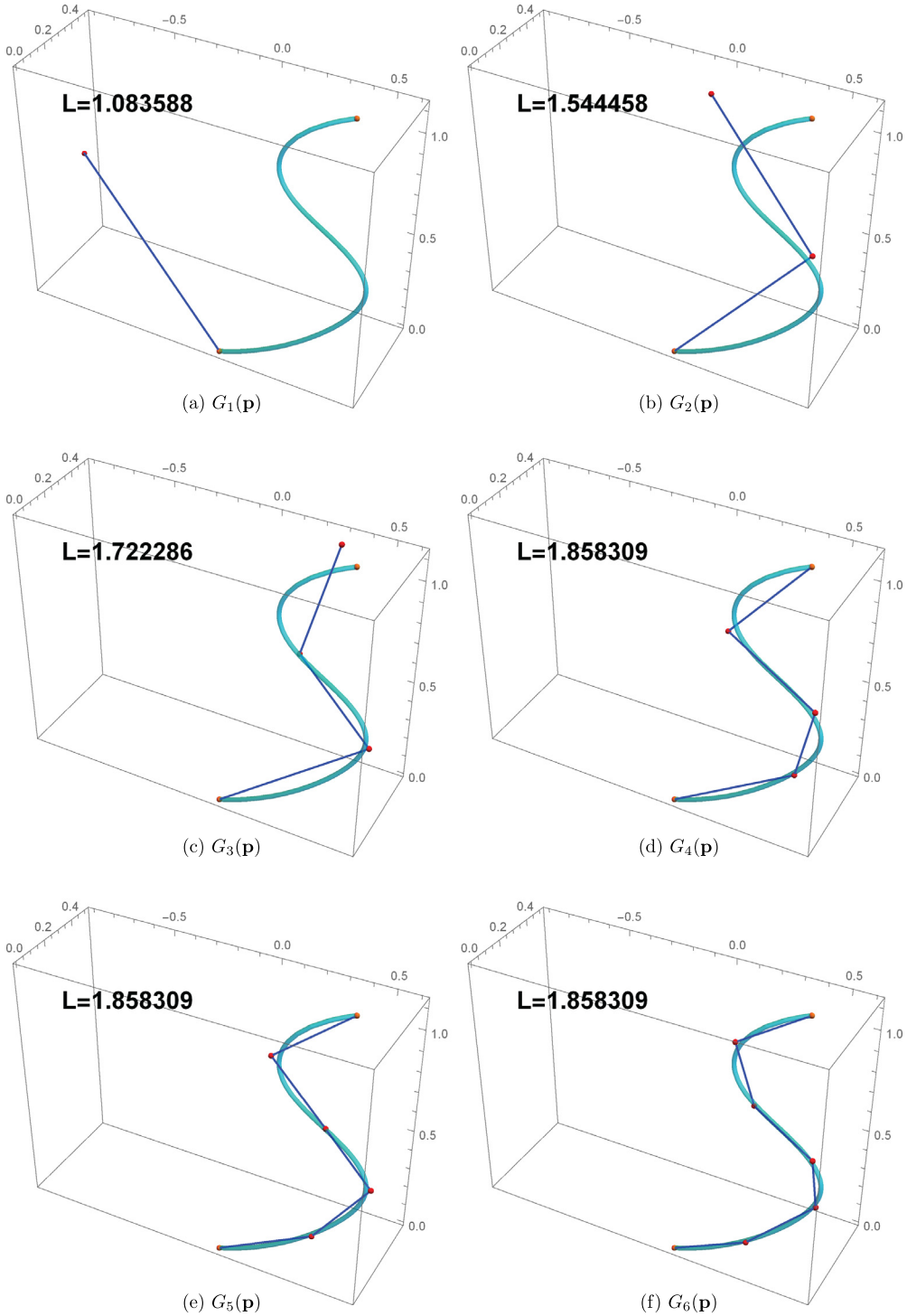

(a) $G_1(\mathbf{p})$ (b) $G_2(\mathbf{p})$

(c) $G_3(\mathbf{p})$ (d) $G_4(\mathbf{p})$

(e) $G_5(\mathbf{p})$ (f) $G_6(\mathbf{p})$

Fig. 2. Gauss–Legendre polygons of the septic PH curve with varying number of nodes. $G_m(\mathbf{p})$ realizes the arc-length of the PH curve for $m \geq 4$.

$$M = \begin{bmatrix} B_0^3\left(\frac{1+\tau_0}{2}\right) & B_1^3\left(\frac{1+\tau_0}{2}\right) & B_2^3\left(\frac{1+\tau_0}{2}\right) & B_3^3\left(\frac{1+\tau_0}{2}\right) \\ B_0^3\left(\frac{1+\tau_1}{2}\right) & B_1^3\left(\frac{1+\tau_1}{2}\right) & B_2^3\left(\frac{1+\tau_1}{2}\right) & B_3^3\left(\frac{1+\tau_1}{2}\right) \\ \vdots & \vdots & \vdots & \vdots \\ B_0^3\left(\frac{1+\tau_4}{2}\right) & B_1^3\left(\frac{1+\tau_4}{2}\right) & B_2^3\left(\frac{1+\tau_4}{2}\right) & B_3^3\left(\frac{1+\tau_4}{2}\right) \end{bmatrix}. \tag{8}$$

Table 1
Nodes and weights of Gauss–Legendre quadrature of order 5.

k	Nodes τ_k	Weights ω_k
0	$-\frac{1}{3}\sqrt{5+2\sqrt{\frac{10}{7}}}$	$\frac{322-13\sqrt{70}}{900}$
1	$-\frac{1}{3}\sqrt{5-2\sqrt{\frac{10}{7}}}$	$\frac{322+13\sqrt{70}}{900}$
2	0	$\frac{128}{225}$
3	$\frac{1}{3}\sqrt{5-2\sqrt{\frac{10}{7}}}$	$\frac{322+13\sqrt{70}}{900}$
4	$\frac{1}{3}\sqrt{5+2\sqrt{\frac{10}{7}}}$	$\frac{322-13\sqrt{70}}{900}$

One may consult Marco and Martìnez (2007) and references therein for more details of the Bernstein–Vandermonte matrix.

Theorem 8. *Suppose a 5 edge polygon $[\mathbf{p}_0\mathbf{p}_1\cdots\mathbf{p}_5]$ is given. The Gauss–Legendre polygon $G_5(\mathbf{p})$ of the septic PH curve $\mathbf{p}$ generated from the cubic quaternion polynomial $\mathcal{A}(t)=\sum_{i=0}^{3}\mathcal{A}_i B_i^3(t)$ agrees with the given polygon $[\mathbf{p}_0\mathbf{p}_1\cdots\mathbf{p}_5]$ if $\mathbf{p}(0)=\mathbf{p}_0$ and the quaternion coefficients of $\mathcal{A}(t)$ satisfy the overdetermined linear system*

$$M\begin{bmatrix}\mathcal{A}_0\\ \mathcal{A}_1\\ \mathcal{A}_2\\ \mathcal{A}_3\end{bmatrix}=\begin{bmatrix}\sqrt[\star]{\frac{2}{\omega_0}\Delta\mathbf{p}_0}\\ \sqrt[\star]{\frac{2}{\omega_1}\Delta\mathbf{p}_1}\,\mathcal{Q}(\phi_1)\\ \sqrt[\star]{\frac{2}{\omega_2}\Delta\mathbf{p}_2}\,\mathcal{Q}(\phi_2)\\ \sqrt[\star]{\frac{2}{\omega_3}\Delta\mathbf{p}_3}\,\mathcal{Q}(\phi_3)\\ \sqrt[\star]{\frac{2}{\omega_4}\Delta\mathbf{p}_4}\,\mathcal{Q}(\phi_4)\end{bmatrix} \tag{9}$$

for some scalar parameters $\phi_1,\cdots,\phi_4$, where $\Delta\mathbf{p}_k=\mathbf{p}_{k+1}-\mathbf{p}_k$.

Proof. The forward differences of $G_5(\mathbf{p})$ are given by

$$\Delta\mathbf{p}_k=\mathbf{p}_{k+1}-\mathbf{p}_k=\frac{\omega_k}{2}\mathbf{p}'\left(\frac{1+\tau_k}{2}\right)=\frac{\omega_k}{2}\mathcal{A}\left(\frac{1+\tau_k}{2}\right)\mathbf{i}\,\mathcal{A}\left(\frac{1+\tau_k}{2}\right)^*,$$

which is equivalent to

$$\mathcal{A}\left(\frac{1+\tau_k}{2}\right)^{2\star}=\frac{2}{\omega_k}\Delta\mathbf{p}_k.$$

The equation can be solved in terms of $\mathcal{A}$ by $\mathcal{A}\left(\frac{1+\tau_k}{2}\right)=\sqrt[\star]{\frac{2}{\omega_k}\Delta\mathbf{p}_k}\,\mathcal{Q}(\phi_k)$ with parameters ϕ_k for $=0,\cdots,4$. Here, $\mathcal{A}\left(\frac{1+\tau_k}{2}\right)=\sum_{i=0}^{3}\mathcal{A}_i B_i^3\left(\frac{1+\tau_k}{2}\right)$ corresponds to each row of the overdetermined linear system (9). Since the quaternion polynomial $\mathcal{A}(t)$ also has a free parameter θ in the form of (7), our system is in fact

$$\mathcal{A}\left(\frac{1+\tau_k}{2}\right)\mathcal{Q}(\theta)=\sqrt[\star]{\frac{2}{\omega_k}\Delta\mathbf{p}_k}\,\mathcal{Q}(\phi_k).$$

By choosing $\theta=\phi_0$ and renaming $\phi_k-\theta$ as ϕ_k for $k=1,\cdots,4$, we get the overdetermined linear system (9). □

In order to construct a septic PH curve $\mathbf{p}$ with the prescribed Gauss–Legendre polygon $G_5(\mathbf{p})=[\mathbf{p}_0\mathbf{p}_1\cdots\mathbf{p}_5]$, we need to make the linear system (9) solvable by choosing the parameters ϕ_1, ϕ_2, ϕ_3, ϕ_4 elaborately. Although the linear system (9) consists of equations of quaternion values and unknowns, the coefficient matrix M is a real matrix. So the scalar part and each $\mathbf{i}$, $\mathbf{j}$, $\mathbf{k}$ parts of the quaternion linear system (9) can be treated separately in the form of real linear system

$$M\mathbf{x}=\mathbf{q}, \tag{10}$$

where $\mathbf{x}$ is an unknown vector in $\mathbb{R}^4$ and $\mathbf{q}$ is a given value in $\mathbb{R}^5$.

To analyze the solvability of the overdetermined system, we exploit the standard theory of the least square solution in linear algebra. One may consult any linear algebra textbook, for example Anton and Busby (2003). The least square solution $\hat{\mathbf{x}}$ of (10) can be obtained by solving the corresponding normal equations

$$M^\top M\mathbf{x} = M^\top \mathbf{q},$$

which yields

$$\hat{\mathbf{x}} = \left(M^\top M\right)^{-1} M^\top \mathbf{q}.$$

Note that $M^\top M$ is invertible since M has a full rank. The matrix $\left(M^\top M\right)^{-1} M^\top$ is called as the pseudo-inverse of M when M has full column rank. The least square error vector $\mathbf{q} - M\hat{\mathbf{x}}$ is then the projection of $\mathbf{q}$ to the null space of $M^\top$. So the least square solution becomes the true solution of the over-determined system (9) if $\mathbf{q}$ is orthogonal to the null space of $M^\top$, which can be identified by the following Lemma.

Lemma 9. *The null space of $M^\top$ for the Bernstein–Vandermonde matrix M, defined in (8), is the 1 dimensional space in $\mathbb{R}^5$ spanned by*

$$\mathbf{m} = (m_0, m_1, m_2, m_3, m_4)^\top \tag{11}$$

where

$$m_0 = m_4 = 27, \quad m_1 = m_3 = -43 - 4\sqrt{70}, \quad m_2 = 32 + 8\sqrt{70}. \tag{12}$$

Proof. Since $rank(M) = 4$, the column space of M is of dimension 4, and $M^\top$ has a 1 dimensional null space. One can easily verify that $\mathbf{m}$ is a solution of $M^\top \mathbf{m} = \mathbf{0}$. □

As the straightforward consequence of this lemma, we can identify the solvability condition of Equation (9).

Corollary 10. *The overdetermined linear system (9) has the quaternion solutions $\mathcal{A}_0$, $\mathcal{A}_1$, $\mathcal{A}_2$, $\mathcal{A}_3$ if*

$$\sum_{k=0}^{4} m_k \sqrt[\star]{\frac{2}{\omega_k}\Delta\mathbf{p}_k}\, \mathcal{Q}(\phi_k) = 0, \tag{13}$$

where m_k's are given in (12) and $\phi_0 = 0$.

The rest of the section is devoted to the method of finding the parameters ϕ_1, ϕ_2, ϕ_3, ϕ_4 that satisfy (13). For a given Gauss–Legendre polygon $[\mathbf{p}_0\mathbf{p}_1\cdots\mathbf{p}_5]$, the coefficient of $\mathcal{Q}(\phi_k)$ in (13) is the fixed pure quaternion $m_k \sqrt[\star]{\frac{2}{\omega_k}\Delta\mathbf{p}_k}$, which we denote as

$$m_k \sqrt[\star]{\frac{2}{\omega_k}\Delta\mathbf{p}_k} = x_k\,\mathbf{i} + y_k\,\mathbf{j} + z_k\,\mathbf{k}. \tag{14}$$

Putting these expressions to (13) yields

$$\sum_{k=0}^{4} (x_k\,\mathbf{i} + y_k\,\mathbf{j} + z_k\,\mathbf{k})\,(\cos\phi_k + \sin\phi_k\,\mathbf{i}) = 0, \tag{15}$$

which can be split into

$$\begin{aligned} &\sum_{k=0}^{4} -x_k \sin\phi_k = 0, \qquad \sum_{k=0}^{4} (y_k\cos\phi_k + z_k\sin\phi_k) = 0, \\ &\sum_{k=0}^{4} x_k \cos\phi_k = 0, \qquad \sum_{k=0}^{4} (z_k\cos\phi_k - y_k\sin\phi_k) = 0. \end{aligned} \tag{16}$$

When ϕ_0 is fixed as 0, the system of equations can be regarded as the linear relations between the trigonometric functions of ϕ_1, ϕ_2 and the trigonometric functions of ϕ_3, ϕ_4. We can organize these relations in the matrix form

$$A\,\Phi_{34} = B\,\Phi_{12} + C,$$

where

$$A = \begin{bmatrix} x_3 & 0 & x_4 & 0 \\ 0 & x_3 & 0 & x_4 \\ z_3 & y_3 & z_4 & y_4 \\ -y_3 & z_3 & -y_4 & z_4 \end{bmatrix}, \quad \Phi_{34} = \begin{bmatrix} \sin\phi_3 \\ \cos\phi_3 \\ \sin\phi_4 \\ \cos\phi_4 \end{bmatrix},$$
$$B = \begin{bmatrix} -x_1 & 0 & -x_2 & 0 \\ 0 & -x_1 & 0 & -x_2 \\ -z_1 & -y_1 & -z_2 & -y_2 \\ y_1 & -z_1 & y_2 & -z_2 \end{bmatrix}, \quad \Phi_{12} = \begin{bmatrix} \sin\phi_1 \\ \cos\phi_1 \\ \sin\phi_2 \\ \cos\phi_2 \end{bmatrix}, \quad C = \begin{bmatrix} 0 \\ -x_0 \\ -y_0 \\ -z_0 \end{bmatrix}. \tag{17}$$

Thus Φ_{34} can be expressed as

$$\phi_{34} = A^{-1}\left(B\,\Phi_{12} + C\right), \tag{18}$$

if the matrix A is invertible.

Lemma 11. *The matrix A in (17) is invertible if and only if $\Delta\mathbf{p}_3$ and $\Delta\mathbf{p}_4$ are not collinear.*

Proof. By direct computation, we get

$$\det(A) = (x_3 y_4 - x_4 y_3)^2 + (x_3 z_4 - x_4 z_3)^2 .$$

Thus A is invertible if and only if the pure quaternions $x_k\,\mathbf{i} + y_k\,\mathbf{j} + z_k\,\mathbf{k} = m_k \sqrt[\star]{\frac{2}{\omega_k}\Delta\mathbf{p}_k}$ for $k = 3, 4$ are not collinear. Since both m_k and ω_k are real constants, the above condition is equivalent to the collinearity of $\sqrt[\star]{\Delta\mathbf{p}_3}$ and $\sqrt[\star]{\Delta\mathbf{p}_4}$, which is equivalent to the collinearity of $\Delta\mathbf{p}_3$ and $\Delta\mathbf{p}_4$. □

From now on, we assume that all adjacent edges of the given polygon $[\mathbf{p}_0\mathbf{p}_1\cdots\mathbf{p}_5]$ are not collinear. So both A and B are invertible. Then the trigonometric functions in Φ_{34} are expressed as the linear combination of the trigonometric functions in Φ_{12} through Equation (18). So if we fix the values of ϕ_1 and ϕ_2, then the other two parameters ϕ_3 and ϕ_4 will be determined. However the values of ϕ_1 and ϕ_2 cannot be chosen arbitrary. They should be selected to fulfill the conditions $\sin^2\phi_3 + \cos^2\phi_3 = \sin^2\phi_4 + \cos^2\phi_4 = 1$. If we denote the entries of $A^{-1}B$ as a_{ij} and the entries of $A^{-1}C$ as b_i, i.e.,

$$A^{-1}B =: \left[a_{ij}\right]_{i,j=1}^{4}, \text{ and } A^{-1}C =: \left[b_i\right]_{i=1}^{4}$$

for $i,\ j = 1, 2, 3, 4$, then the above conditions can be written as

$$\begin{aligned} &\left(a_{11}\sin\phi_1 + a_{12}\cos\phi_1 + a_{13}\sin\phi_2 + a_{14}\cos\phi_2 + b_1\right)^2 \\ &+ \left(a_{21}\sin\phi_1 + a_{22}\cos\phi_1 + a_{23}\sin\phi_2 + a_{24}\cos\phi_2 + b_2\right)^2 = 1, \\ &\left(a_{31}\sin\phi_1 + a_{32}\cos\phi_1 + a_{33}\sin\phi_2 + a_{34}\cos\phi_2 + b_3\right)^2 \\ &+ \left(a_{41}\sin\phi_1 + a_{42}\cos\phi_1 + a_{43}\sin\phi_2 + a_{44}\cos\phi_2 + b_4\right)^2 = 1. \end{aligned} \tag{19}$$

So ϕ_1 and ϕ_2 are the solutions of the system of trigonometric equations. There are many efficient algorithms to compute the solutions of the nonlinear system like (19). For example, the Newton–Raphson method with approximate initial guess gives quadratic convergence to the solution. One may consult Burden and Faires (1989) for the details of the multivariable Newton–Raphson method.

Remark 12. The above nonlinear system of equations cannot be solved exactly only with symbolic computation. It is inevitable to rely on any kind of numerical approximation at some stage of the computation. This numerical error in the approximation hinders the perfect match between the lengths of the PH curve and the Gauss–Legendre polygon. The accuracy of solutions of (19) affects the accuracy of the length match. In fact, we cannot fully avoid the issue of numerical approximation error in the most practical computation. Even simple functions, such as `sqrt`, are implemented by using the Newton method in the mathematical libraries of many programming languages. Thus we cannot compute the *exact* length of a single line segment using `sqrt` function. Although the present approach using numerical approximation can be regarded not adequate for the exactness of PH curves, we think that the proposed method still have valid applications in the practice.

Another way to solve Equation (19) is by using the resultant. We can convert Equation (19) into the system of *polynomial* equations by introducing new variables $t_i = \tan\frac{\phi_i}{2}$ for $i = 1, 2$. Since $\sin\phi_i = 2t_i/(1+t_i^2)$ and $\cos\phi_i = (1-t_i^2)/(1+t_i^2)$, the system (19) becomes

Table 2
Common roots for t_1, t_2 and the corresponding parameters ϕ_1, ϕ_2, ϕ_3, ϕ_4.

Solution	t_1	t_2	ϕ_1	ϕ_2	ϕ_3	ϕ_4
(a)	0.300325	−1.157858	−0.583509	−1.716846	−1.717898	−1.203628
(b)	0.299491	−0.551772	0.581979	−1.008405	−1.111215	1.287224
(c)	−0.376098	0.055981	−0.719465	0.111845	0.379552	−1.435949
(d)	0.316375	0.755315	0.612823	1.293789	1.680993	1.504541

$$
\begin{aligned}
f(t_1,t_2) :=& \Big[\big(2a_{11}t_1 + a_{12}(1-t_1^2)\big)(1+t_2^2) + \big(2a_{13}t_2 + a_{14}(1-t_2^2)\big)(1+t_1^2) + b_1(1+t_1^2)(1+t_2^2)\Big]^2 \\
&+ \Big[\big(2a_{21}t_1 + a_{22}(1-t_1^2)\big)(1+t_2^2) + \big(2a_{23}t_2 + a_{24}(1-t_2^2)\big)(1+t_1^2) + b_2(1+t_1^2)(1+t_2^2)\Big]^2 \\
&- (1+t_1^2)^2(1+t_2^2)^2 = 0, \\
g(t_1,t_2) :=& \Big[\big(2a_{31}t_1 + a_{32}(1-t_1^2)\big)(1+t_2^2) + \big(2a_{33}t_2 + a_{34}(1-t_2^2)\big)(1+t_1^2) + b_3(1+t_1^2)(1+t_2^2)\Big]^2 \\
&+ \Big[\big(2a_{41}t_1 + a_{42}(1-t_1^2)\big)(1+t_2^2) + \big(2a_{43}t_2 + a_{44}(1-t_2^2)\big)(1+t_1^2) + b_4(1+t_1^2)(1+t_2^2)\Big]^2 \\
&- (1+t_1^2)^2(1+t_2^2)^2 = 0.
\end{aligned}
\tag{20}
$$

The whole problem now turns into the bivariate polynomial system $f(t_1,t_2) = g(t_1,t_2) = 0$. The common root of this polynomial system can be computed by using the resultant. One may consult Farouki (2008) for more details of the resultant based method for polynomial system.

Suppose $(\hat{t}_1, \hat{t}_2)$ is a common root of $f(t_1,t_2) = g(t_1,t_2) = 0$. The corresponding angular parameters can be obtained by

$$
\phi_1 = 2\tan^{-1} t_1, \qquad \phi_2 = 2\tan^{-1} t_2. \tag{21}
$$

By putting these values to Equation (18), we get the values of $\sin\phi_3$, $\cos\phi_3$, $\sin\phi_4$, and $\cos\phi_4$. We need to use some caution in converting these values to the angular parameters ϕ_3 and ϕ_4. For given values of $\sin\phi_i$ and $\cos\phi_i$, the angle ϕ_i can be obtained by either

$$
\phi_i = \sin^{-1}(\sin\phi_i) \quad \text{or} \quad \phi_i = \cos^{-1}(\cos\phi_i).
$$

However neither of these expressions can recover ϕ_i in the full range $(-\pi, \pi)$. The numerical stabilities of the functions $\sin^{-1}$ and $\cos^{-1}$ are also different depending on the value of ϕ_i. Both $\sin^{-1} t$ and $\cos^{-1} t$ have less stability when $|t|$ is close to 1. So we suggest using different functions depending on the range of ϕ_i given by

$$
\phi_i = \begin{cases}
\sin^{-1}(\sin\phi_i) & \text{if } \cos\phi_i \geq |\sin\phi_i|, \\
\pi - \sin^{-1}(\sin\phi_i) & \text{if } \sin\phi_i \geq 0,\ \cos\phi_i < -\sin\phi_i, \\
-\pi - \sin^{-1}(\sin\phi_i) & \text{if } \sin\phi_i < 0,\ \cos\phi_i < \sin\phi_i, \\
\cos^{-1}(\cos\phi_i) & \text{if } \sin\phi_i \geq |\cos\phi_i|, \\
-\cos^{-1}(\cos\phi_i) & \text{if } \sin\phi_i \leq -|\cos\phi_i|.
\end{cases} \tag{22}
$$

The angular parameters ϕ_i for $i = 1,2,3,4$ make the over-determined system (9) solvable. The quaternion solution $\mathcal{A}_0$, $\mathcal{A}_1$, $\mathcal{A}_2$, $\mathcal{A}_3$ can be obtained by solving the overdetermined system (9). The Bézier control points of the resulting septic PH curve can then be computed by (5). The following example illustrates the septic PH curves with prescribed Gauss–Legendre polygon computed by this procedure.

Example 13. Suppose a rectifying polygon $[\mathbf{p}_0 \cdots \mathbf{p}_5]$ is given by

$$
\begin{aligned}
\mathbf{p}_0 &= 0, & \mathbf{p}_3 &= 0.35\,\mathbf{i} + 0.25\,\mathbf{j} + 0.6\,\mathbf{k}, \\
\mathbf{p}_1 &= 0.4\,\mathbf{i} + 0.05\,\mathbf{j} + 0.2\,\mathbf{k}, & \mathbf{p}_4 &= 0.05\,\mathbf{i} + 0.35\,\mathbf{j} + 0.8\,\mathbf{k}, \\
\mathbf{p}_2 &= 0.6\,\mathbf{i} + 0.15\,\mathbf{j} + 0.45\,\mathbf{k}, & \mathbf{p}_5 &= 0.35\,\mathbf{i} + 0.5\,\mathbf{j} + 1.0\,\mathbf{k}.
\end{aligned}
$$

The computation using resultant produces 4 pairs of common roots of the system (20). Those common roots for (t_1,t_2) and the corresponding parameters $\phi_1, \phi_2, \phi_3, \phi_4$ are listed in Table 2.

Fig. 3 illustrates the septic PH curves generated by each set of parameters in Table 2. The green polygons in each plot are the Bézier polygons of the PH curves. Although their Bézier polygons look very different in shape, the PH curves are close to each other as shown in Fig. 3 (e). This is because the rectifying control polygon confines the arc length and the tangent vectors at 5 Gauss–Legendre nodes $\tau_{5,k}$.

5. Solvability analysis

We presented the computational technique for finding spatial septic PH curves with the prescribed Gauss–Legendre polygon. During the numerical experiments, we discovered that not all the Gauss–Legendre polygon have the corresponding septic PH curve. For some wild-varying polygons, the resultant does not have any real root. According to our experiment, the number of PH curves for any given Gauss–Legendre polygon varies in $\{0, 2, 4, 6\}$. It seems that the classification of the Gauss–Legendre polygons based on the number of solutions are very difficult because of the highly nonlinear nature of the problem. Hence, in this paper, we investigate a few conditions for the existence of the solutions.

In the previous algorithm, we split Equation (15) into the system of 4 real equations as in (16). Equation (15) can also be treated as the system of 2 complex equations. From

$$\sum_{k=0}^{4} (x_k\,\mathbf{i} + y_k\,\mathbf{j} + z_k\,\mathbf{k})\, e^{\mathbf{i}\phi_k} = \sum_{k=0}^{4} x_k\,\mathbf{i} e^{\mathbf{i}\phi_k} + \sum_{k=0}^{4} (y_k\,\mathbf{j} + z_k\,\mathbf{k})\, e^{\mathbf{i}\phi_k},$$

the former sum has only the real and $\mathbf{i}$ components, and the latter sum has only the $\mathbf{j}$ and $\mathbf{k}$ components. By multiplying $-\mathbf{i}$ and $-\mathbf{k}$ to each summations, we get the system of two complex equations

$$\sum_{k=0}^{4} x_k e^{\mathbf{i}\phi_k} = 0, \tag{23}$$

$$\sum_{k=0}^{4} (z_k + y_k\,\mathbf{i})\, e^{\mathbf{i}\phi_k} = \sum_{k=0}^{4} r_k e^{\mathbf{i}(\phi_k+\psi_k)} = 0, \tag{24}$$

where $r_k = \sqrt{y_k^2 + z_k^2}$ and

$$\psi_k = \begin{cases} \tan^{-1}(y_k/z_k) & \text{if } z_k > 0, \\ \operatorname{sgn}(y_k)\pi/2 & \text{if } z_k = 0, \\ \tan^{-1}(y_k/z_k) + \pi & \text{if } z_k < 0. \end{cases}$$

This system may have solutions only if each individual equation has solutions. We here present a necessary condition for the existence of the solutions of Equations (24). Equation (23) can be treated as a special case of Equation (24) with all values of ψ_k chosen as zeros.

Theorem 14. *For given r_k and ψ_k, Equation (24) can have solutions only if*

$$2 \max_{0\le k\le 4} |r_k| \le \sum_{k=0}^{4} |r_k|\,. \tag{25}$$

Proof. Let us assume $|r_k|$ attains the maximum when $k = k_0$, i.e., $|r_{k_0}| = \max_{0\le k\le 4} |r_k|$. From Equation (24), we get

$$r_{k_0} e^{\mathbf{i}\left(\phi_{k_0}+\psi_{k_0}\right)} = -\sum_{k\neq k_0} r_k e^{\mathbf{i}(\phi_k+\psi_k)}.$$

By the triangle inequality, we can derive

$$\max_{0\le k\le 4} |r_k| = |r_{k_0}| = \left| \sum_{k\neq k_0} r_k e^{\mathbf{i}(\phi_k+\psi_k)} \right| \le \sum_{k\neq k_0} |r_k|,$$

which can be formulated as (25). □

By the same reason, Equation (23) can have solutions only if

$$2 \max_{0\le k\le 4} |x_k| \le \sum_{k=0}^{4} |x_k|\,. \tag{26}$$

If either (25) or (26) is not true, the whole system does not have a solution. Thus we no longer have to proceed the Newton method of the algorithm to solve the problem. The following is the example that does not have a solution because it fails to satisfy (25).

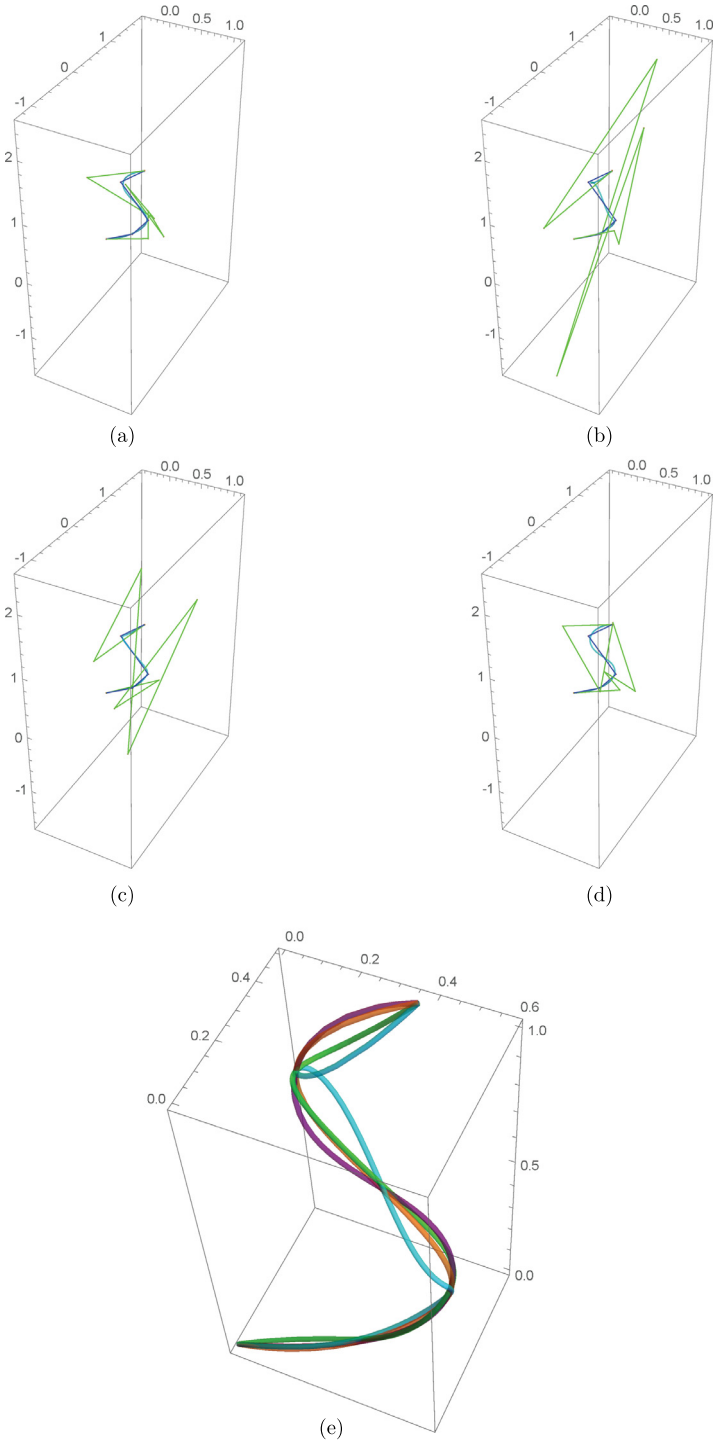

Fig. 3. (a)–(d) Four different septic PH curves are illustrated with their Bézier polygon, (e) Four septic PH curves are shown together.

Example 15. Suppose a polygon $[\mathbf{p}_0 \cdots \mathbf{p}_5]$ is given by

$$\mathbf{p}_0 = \quad 0,$$
$$\mathbf{p}_1 = -0.757472\,\mathbf{i} + 0.091006\,\mathbf{j} - 0.459571\,\mathbf{k},$$
$$\mathbf{p}_2 = -1.487811\,\mathbf{i} + 0.176687\,\mathbf{j} - 0.403849\,\mathbf{k},$$

$$\mathbf{p}_3 = -1.886010\,\mathbf{i} + 0.582306\,\mathbf{j} - 0.425481\,\mathbf{k},$$
$$\mathbf{p}_4 = -1.387375\,\mathbf{i} + 0.286333\,\mathbf{j} - 1.174156\,\mathbf{k},$$
$$\mathbf{p}_5 = -1.938066\,\mathbf{i} - 0.012520\,\mathbf{j} - 1.153471\,\mathbf{k}.$$

The corresponding values for x_k are

$$x_0 = 0.133651, x_1 = -0.061563, x_2 = 0.357724, x_3 = -0.877405, x_4 = 0.101102.$$

The absolute value of x_3 is too large and the condition (25) is not satisfied since $2\max_{0\le k\le 4}|x_k| = 2|x_3| = 1.754810 > \sum_{k=0}^{4}|x_k| = 1.531444$. So this polygon is not a Gauss–Legendre polygon of a septic PH curve.

In our algorithm we substitute the trigonometric functions in ϕ_3 and ϕ_4 by the functions in variables ϕ_1 and ϕ_2 using Equation (18). By solving (19) we obtain the solutions ϕ_1 and ϕ_2, which then by (18) determine the solutions values of ϕ_3 and ϕ_4. Moreover, for each complex equation (23) and (24), the choice of ϕ_1 and ϕ_2 affects the existence of the corresponding solutions for ϕ_3 and ϕ_4. The next theorem reveals the conditions on ϕ_1 and ϕ_2 for the existence of the solutions ϕ_3 and ϕ_4 of the Equation (24).

Theorem 16. *For given r_k and ψ_k, we fix $\phi_0 = 0$ and choose values for ϕ_1 and ϕ_2. Equation (24) has solutions for ϕ_3 and ϕ_4 if and only if*

$$\big||r_3| - |r_4|\big| \le r_5(\phi_1, \phi_2) \le |r_3| + |r_4|, \tag{27}$$

where

$$r_5(\phi_1, \phi_2) = \left| r_0 e^{\mathbf{i}\psi_0} + r_1 e^{\mathbf{i}(\phi_1+\psi_1)} + r_2 e^{\mathbf{i}(\phi_2+\psi_2)} \right|. \tag{28}$$

Proof. With the fixed ϕ_1 and ϕ_2, we express the sum of three fixed terms in (24) as the polar coordinate

$$r_5 e^{\mathbf{i}\psi_5} := r_0 e^{\mathbf{i}\psi_0} + r_1 e^{\mathbf{i}(\phi_1+\psi_1)} + r_2 e^{\mathbf{i}(\phi_2+\psi_2)}.$$

Equation (24) can then be written as

$$r_3 e^{\mathbf{i}(\phi_3+\psi_3)} + r_4 e^{\mathbf{i}(\phi_4+\psi_4)} + r_5 e^{\mathbf{i}\psi_5} = 0.$$

The solutions for ϕ_3 and ϕ_4 exist if and only if we can build the triangle with the edges of the lengths $|r_3|$, $|r_4|$, $|r_5|$. The triangle inequality for these numbers can be formulated as (27). □

Similarly, Equation (23) has solutions for ϕ_3 and ϕ_4 if and only if

$$\big||x_3| - |x_4|\big| \le x_5(\phi_1, \phi_2) \le |x_3| + |x_4| \tag{29}$$

where $x_5(\phi_1, \phi_2) = \left|x_0 + x_1 e^{\mathbf{i}\phi_1} + x_2 e^{\mathbf{i}\phi_2}\right|$. The magnitude r_5 defined in (28) is a function of two variables ϕ_1 and ϕ_2. If we plot $r_5(\phi_1, \phi_2)$ on the square domain

$$\left\{(\phi_1, \phi_2)\,\middle|\, -\pi \le \phi_1 \le \pi,\ -\pi \le \phi_2 \le \pi\right\},$$

then the set of feasible points (ϕ_1, ϕ_2) can be identified by (27). If we compute the feasible sets of ϕ_1 and ϕ_2 for both (23) and (24), then the solution can appear only in the intersection of these two feasible sets. The following example illustrates the feasible sets for a particular polygon.

Example 17. We investigate the feasible set of ϕ_1 and ϕ_2 for the Gauss–Legendre control polygon in Example 13. Each edge $\Delta\mathbf{p}_k$ of the polygon is converted into the pure quaternion $x_k\,\mathbf{i} + y_k\,\mathbf{j} + z_k\,\mathbf{k}$ by (14). The values of x_k, y_k, and z_k are listed in Table 3. To identify the feasible set given by (29), we generate the contour plot of the function $x_5(\phi_1, \phi_2)$ as shown in Fig. 4 (a). The feasible set is the region between two level curves $x_5(\phi_1, \phi_2) = \big||x_3| - |x_4|\big| = 0.105595$ and $x_5(\phi_1, \phi_2) = |x_3| + |x_4| = 0.503067$, which are plotted as the thick dotted line and the thick solid line, respectively. This feasible set is illustrated as the red region in Fig. 4 (b). We also compute the feasible set for (24) using $r_5(\phi_1, \phi_2)$ in (28). This feasible set is illustrated as the blue region in Fig. 4 (c). Thus the solution of (ϕ_1, ϕ_2) should appear in the intersection of two feasible sets. Fig. 4 (d) shows the overlap of two feasible sets. The solutions of (ϕ_1, ϕ_2) that correspond to the 4 septic PH curves in Example 13 are plotted as the yellow points. All these points are located in the intersection of two feasible sets, which is the purple region in Fig. 4 (d).

Table 3
The variables for the solvability analysis of Example 17 are listed.

k	x_k	y_k	z_k	r_k	ψ_k
0	0.337653	0.019862	0.079448	0.081893	0.244979
1	−0.533972	−0.099731	−0.249329	0.268535	3.522099
2	0.208963	0.358915	0.538373	0.647044	0.588003
3	−0.198736	−0.267962	−0.535925	0.599182	3.605240
4	0.304331	0.066110	0.088146	0.110183	0.643501

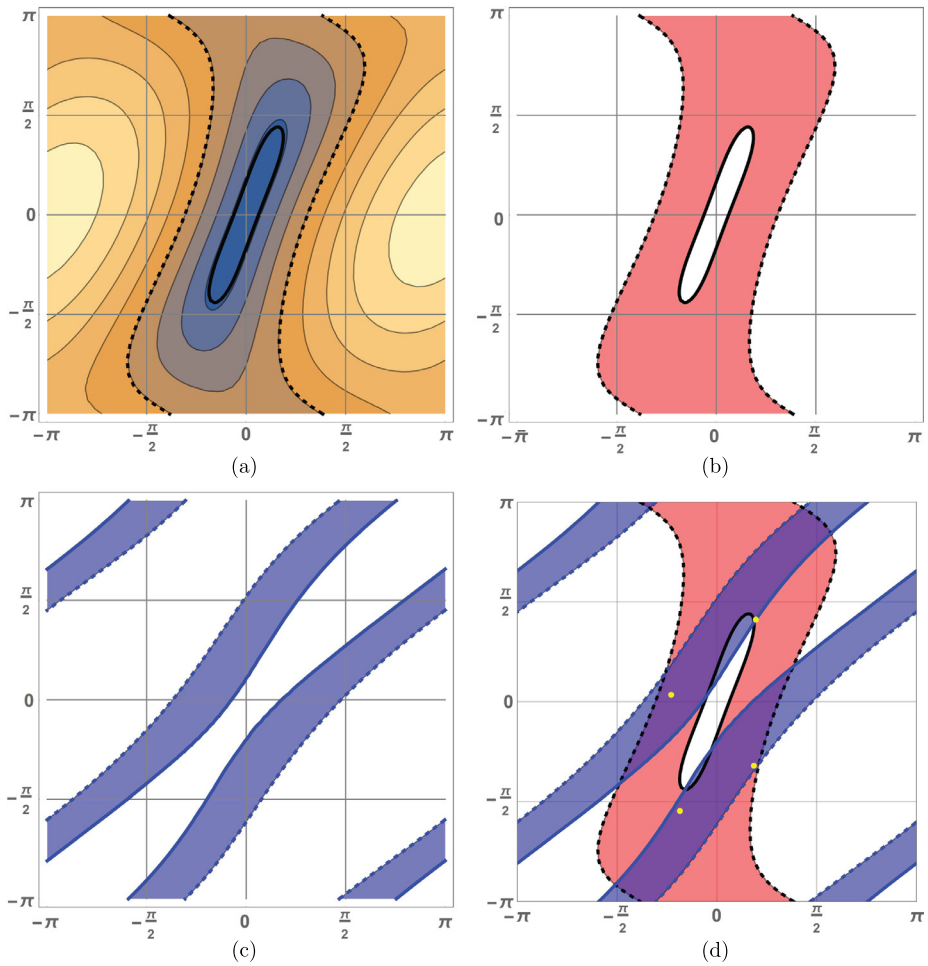

Fig. 4. (a) The contour plot of $x_5(\phi_1, \phi_2)$ is shown together with level curves corresponding to $\big||x_3| - |x_4|\big|$ and $|x_3| + |x_4|$. (b) The red region is the feasible set for (23). (c) The blue region is the feasible set for (24). (d) The yellow points indicate the solution of (ϕ_1, ϕ_2).

The solution (ϕ_1, ϕ_2) should be located in the intersection of two feasible sets given by (27) and (29). If the intersection is empty, then the problem does not have a solution. If we have a nonempty feasible set, we can utilize this information to guide the Newton iteration method for the system (19). It is better to choose the initial point of the Newton method inside the feasible set. We can also check whether the Newton iteration point stays in the feasible set. If the iteration point moves out of the feasible set, then we stop the iteration and start from another initial guess.

6. Deformation of spatial septic PH curves

We here develop the deformation algorithm for spatial septic PH curves using Gauss–Legendre polygon. Suppose we are given a septic PH curve and want to modify its shape for design purpose. We cannot move its Bézier control points because the modification of the Bézier control points results in the violation of the PH property. We use the Gauss–Legendre polygon instead to control the shape of the septic PH curve.

Algorithm 1: Deformation of spatial septic PH curve.

Data: a septic PH curve $\mathbf{p}(t)$ with the Bézier control points $\mathbf{b}_0, \cdots, \mathbf{b}_7$, and the Gauss–Legendre polygon $G_5(\mathbf{p}) = [\mathbf{p}_0 \cdots \mathbf{p}_5]$.
Input: the modified Gauss–Legendre polygon $[\widetilde{\mathbf{p}}_0 \cdots \widetilde{\mathbf{p}}_5]$.

1. compute the $\star$-square roots $\sqrt[\star]{\frac{2}{\omega_k}\Delta\widetilde{\mathbf{p}}_k}$ where $\Delta\widetilde{\mathbf{p}}_k = \widetilde{\mathbf{p}}_{k+1} - \widetilde{\mathbf{p}}_k$ and $\omega_k = \omega_{5,k}$ are the weights of Gauss–Legendre quadrature of order 5 given in Table 1;
2. express $m_k\sqrt[\star]{\frac{2}{\omega_k}\Delta\widetilde{\mathbf{p}}_k}$ as a pure vector $x_k\mathbf{i} + y_k\mathbf{j} + z_k\mathbf{k}$ for m_k in (12);
3. construct the matrices A, B, C in (17);
4. evaluate $[a_{ij}] = A^{-1}B$, and $[b_i] = A^{-1}C$;
5. determine the angular parameters ϕ_1, ϕ_2 by using the Newton method to Equation (19) with the initial guess in $G_5(\mathbf{p})$;
6. evaluate $\sin\phi_3$, $\cos\phi_3$, $\sin\phi_4$, $\cos\phi_4$ by (18);
7. determine the angular parameters ϕ_3, ϕ_4 by (22);
8. solve the overdetermined system;
9. use the solution $\widetilde{\mathcal{A}}_0$, $\widetilde{\mathcal{A}}_1$, $\widetilde{\mathcal{A}}_2$, $\widetilde{\mathcal{A}}_3$ to get the Bézier control points $\hat{\mathbf{b}}_0, \cdots, \hat{\mathbf{b}}_7$ by (5);

Output: a septic PH curve $\widetilde{\mathbf{p}}(t)$ with the Gauss–Legendre polygon $\widetilde{G}_5(\widetilde{\mathbf{p}})$.

Let $\mathbf{p}(t)$ be the spatial septic PH curve defined by the cubic quaternion polynomial $\mathcal{A}(t)$ as its preimage. We first compute the Gauss–Legendre polygon $G_5(\mathbf{p}) = [\mathbf{p}_0 \cdots \mathbf{p}_5]$, which has both rectifying and end point interpolation property by Theorem 4 and Theorem 5. To change the shape of $\mathbf{p}(t)$, we modify the Gauss–Legendre polygon to $[\widetilde{\mathbf{p}}_0 \cdots \widetilde{\mathbf{p}}_5]$, then compute the septic PH curve whose Gauss–Legendre polygon agree with $[\widetilde{\mathbf{p}}_0 \cdots \widetilde{\mathbf{p}}_5]$. Although there might be multiple PH curves with the Gauss–Legendre polygon $[\widetilde{\mathbf{p}}_0 \cdots \widetilde{\mathbf{p}}_5]$, we prefer the one that is closest to the original PH curve. The Newton method with the initial guess obtained from the original curve is well-suited for this purpose if the change of the Gauss–Legendre polygon is minute. For the convenience of the readers, we here summarize the deformation procedure of septic PH curves in Algorithm 1.

When the final Gauss–Legendre polygon is quite different from the original one, a single-step Newton method may result in an undesired solution. In such a case, we propose to use a homotopy method.

Let $[\mathbf{p}_0\mathbf{p}_1 \cdots \mathbf{p}_5]$ and $[\widetilde{\mathbf{p}}_0\widetilde{\mathbf{p}}_1 \cdots \widetilde{\mathbf{p}}_5]$ be the initial and the final Gauss–Legendre polygons respectively. These two polygons can be linked by the homotopy of polygons $[\mathbf{q}_0(u)\mathbf{q}_1(u) \cdots \mathbf{q}_5(u)]$ where $\mathbf{q}_i(u) = (1-u)\mathbf{p}_i + u\widetilde{\mathbf{p}}_i$ for $i = 0, \cdots, 5$. By choosing discrete samples u_k for $k = 0, \cdots, N$ such that $0 = u_0 < u_1 < \cdots < u_N = 1$, we get a sequence of polygons moving from the initial Gauss–Legendre polygon to the final Gauss–Legendre polygon. Then we apply the previous algorithm to each step from $[\mathbf{q}_0(u_k)\mathbf{q}_1(u_k) \cdots \mathbf{q}_5(u_k)]$ to $[\mathbf{q}_0(u_{k+1})\mathbf{q}_1(u_{k+1}) \cdots \mathbf{q}_5(u_{k+1})]$ successively.

We here present an illustrative example of the deformation process of septic PH curves. The following example shows the behavior of the solutions computed by the homotopy method.

Example 18. We start from the PH curve in Example 6, whose Gauss–Legendre polygon $[\mathbf{p}_0 \cdots \mathbf{p}_5]$ is given by

$$\begin{aligned} \mathbf{p}_0 &= 0, & \mathbf{p}_3 &= 0.35\,\mathbf{i} + 0.25\,\mathbf{j} + 0.6\,\mathbf{k}, \\ \mathbf{p}_1 &= 0.4\,\mathbf{i} + 0.05\,\mathbf{j} + 0.2\,\mathbf{k}, & \mathbf{p}_4 &= 0.05\,\mathbf{i} + 0.35\,\mathbf{j} + 0.8\,\mathbf{k}, \\ \mathbf{p}_2 &= 0.6\,\mathbf{i} + 0.15\,\mathbf{j} + 0.45\,\mathbf{k}, & \mathbf{p}_5 &= 0.35\,\mathbf{i} + 0.5\,\mathbf{j} + 1.0\,\mathbf{k}. \end{aligned}$$

The final Gauss–Legendre polygon is chosen as

$$\begin{aligned} \widetilde{\mathbf{p}}_0 &= 0, & \widetilde{\mathbf{p}}_3 &= 0.05\,\mathbf{i} + 0.3\,\mathbf{j} + 0.6\,\mathbf{k}, \\ \widetilde{\mathbf{p}}_1 &= 0.37\,\mathbf{i} + 0.1\,\mathbf{j} + 0.2\,\mathbf{k}, & \widetilde{\mathbf{p}}_4 &= 0.2\,\mathbf{i} + 0.01\,\mathbf{j} + 0.8\,\mathbf{k}, \\ \widetilde{\mathbf{p}}_2 &= 0.3\,\mathbf{i} + 0.37\,\mathbf{j} + 0.395\,\mathbf{k}, & \widetilde{\mathbf{p}}_5 &= 0.5\,\mathbf{i} + 1.0\,\mathbf{k}. \end{aligned}$$

We then subdivide the motion between the original and the final Gauss–Legendre polygons by 8 homotopic steps. Fig. 5 (a) shows the initial and final septic PH curves with their Gauss–Legendre polygon in red and purple curves, respectively. Fig. 5 (b) shows the same data from another viewpoint, which is from the right side of (a). By the homotopy method, we constructed a set of polygons shown in Fig. 5 (c). We then applied the previous algorithm to each step, which results in the set of septic PH curves shown in Fig. 5 (d).

7. Closure and future work

The notion of rectifying polygon of planar PH curves (Kim and Moon, 2017) was extended to spatial PH curves. It was shown that the Gauss–Legendre polygon with sufficiently many edges realized the arc length of a spatial PH curve. We also presented the method of controlling spatial PH curve by manipulating its Gauss–Legendre polygon. We developed the algorithm to compute septic PH curves from a given Gauss–Legendre polygon with 5 edges. The number of septic PH curves with given Gauss–Lengendre polygon may vary depending on the polygon. We investigated a few necessary conditions for the existence of the solutions. We also proposed the selection scheme out of multiple solutions in the context of

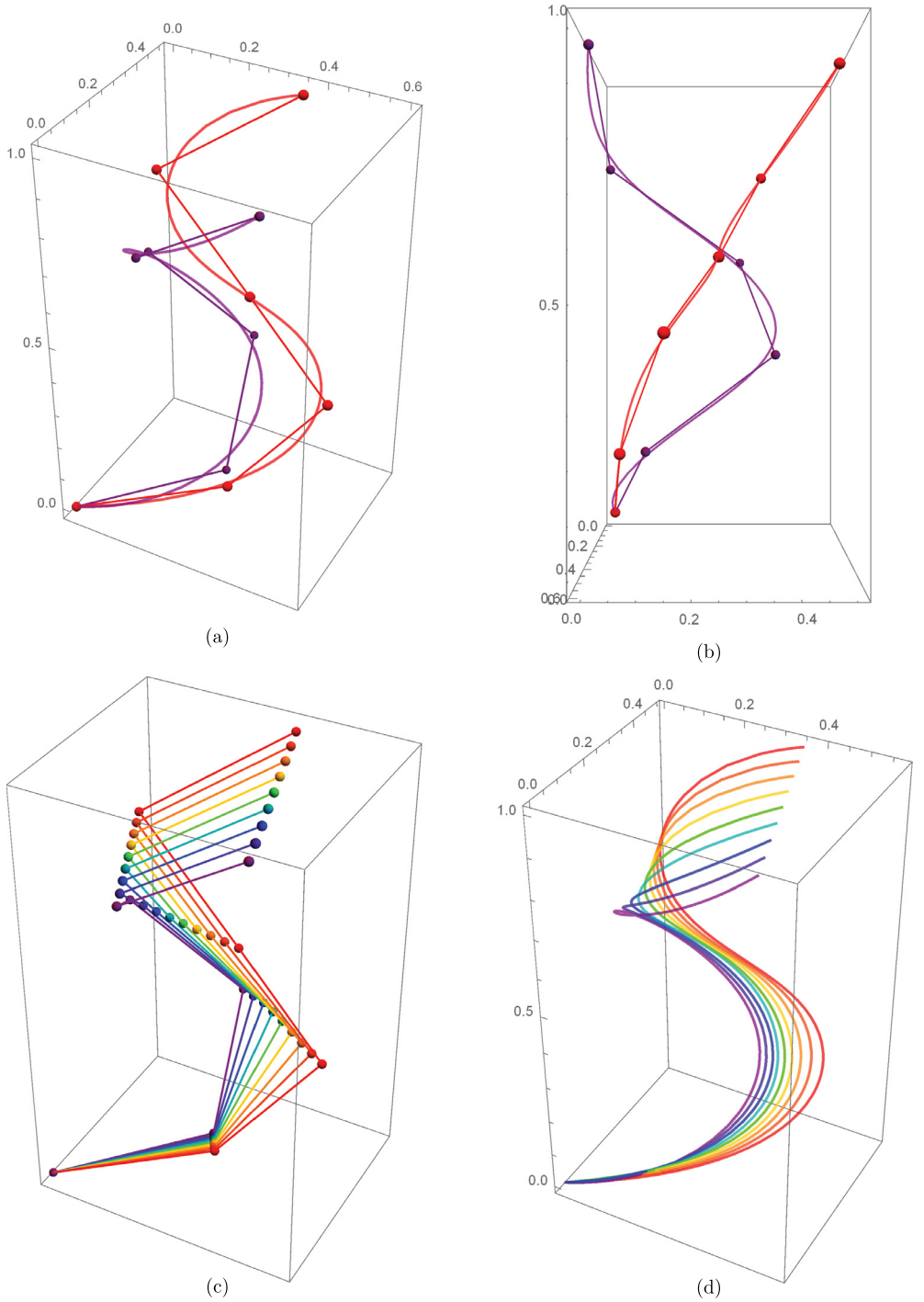

Fig. 5. (a) The initial and the final septic PH curves with their Gauss–Legendre polygons are shown in red and purple curves, respectively. (b) The same data in (a) are shown from another viewpoint. (c) The discrete samples from the homotopy of polygons are shown in lines with increasing hue value. (d) The set of septic PH curves obtained by applying the proposed algorithm to each step are shown as the curves of the same color with the corresponding polygon in (c).

modification of an original septic PH curve. We presented a worked-out example of a deformation of a septic PH curve using homotopy method.

We think the proposed method is useful to deform a septic PH curve into the desired shape if the existence of solutions is guaranteed, which is true for many cases. The solvability issue is a main obstacle to apply the method to *all* possible polygons. To overcome this problem, we think it is necessary to relax the condition on the degree of freedom. If we allow

more degrees of freedom for the PH curve than the Gauss–Legendre polygon, then we could resolve the solvability problem. But we will have same auxiliary variables which has to be determined by some optimization process. We will address this problem as our future work.

Declaration of Competing Interest

No conflict of interest.

References

Anton, H., Busby, R.C., 2003. Contemporary Linear Algebra. Wiley.
Burden, R.L., Faires, J.D., 1989. Numerical Analysis. Kent Publishing Co., Boston.
Choi, H.I., Farouki, R.T., Kwon, S.H., Moon, H.P., 2008. Topological criterion for selection of quintic Pythagorean-hodograph Hermite interpolants. Comput. Aided Geom. Des. 25 (6), 411–433.
Choi, H.I., Kwon, S.H., 2008. Absolute hodograph winding number and planar PH quintic splines. Comput. Aided Geom. Des. 25 (4–5), 230–246.
Choi, H.I., Lee, D.S., Moon, H.P., 2002. Clifford algebra, spin representation, and rational parameterization of curves and surfaces. Adv. Comput. Math. 17 (1–2), 5–48.
Farouki, R.T., 1994. The conformal map $\mathbf{z} \rightarrow \mathbf{z}^2$ of the hodograph plane. Comput. Aided Geom. Des. 11 (4), 363–390.
Farouki, R.T., 2008. Pythagorean-Hodograph Curves: Algebra and Geometry Inseparable. Springer.
Farouki, R.T., 2016. Construction of G^1 planar Hermite interpolants with prescribed arc lengths. Comput. Aided Geom. Des. 46, 64–75.
Farouki, R.T., al Kandari, M., Sakkalis, T., 2002. Hermite interpolation by rotation-invariant spatial Pythagorean-hodograph curves. Adv. Comput. Math. 17 (4), 369–383.
Farouki, R.T., Giannelli, C., Manni, C., Sestini, A., 2008. Identification of spatial PH quintic Hermite interpolants with near-optimal shape measures. Comput. Aided Geom. Des. 25 (4–5), 274–297.
Farouki, R.T., Neff, C.A., 1995. Hermite interpolation by Pythagorean hodograph quintics. Math. Comput. 64 (212), 1589–1609.
Farouki, R.T., Sakkalis, T., 1990. Pythagorean hodographs. IBM J. Res. Dev. 34, 736–752.
Farouki, R.T., Sakkalis, T., 1994. Pythagorean-hodograph space curves. Adv. Comput. Math. 2 (1), 41–66.
Farouki, R.T., Sakkalis, T., 2007. Rational space curves are not “unit speed”. Comput. Aided Geom. Des. 24 (4), 238–240.
Huard, M., Farouki, R.T., Sprynski, N., Biard, L., 2014. C^2 interpolation of spatial data subject to arc-length constraints using Pythagorean–hodograph quintic splines. Graph. Models 76 (1), 30–42.
Hungerford, T.W., 1974. Algebra. Springer-Verlag, New York.
Jüttler, B., 2001. Hermite interpolation by Pythagorean hodograph curves of degree seven. Math. Comput. 70 (235), 1089–1111.
Kim, S.H., Moon, H.P., 2017. Rectifying control polygon for planar Pythagorean hodograph curves. Comput. Aided Geom. Des. 54, 1–14.
Kwon, S.H., 2010. Solvability of G^1 Hermite interpolation by spatial Pythagorean-hodograph cubics and its selection scheme. Comput. Aided Geom. Des. 27 (2), 138–149.
Marco, A., Martìnez, J.-J., 2007. A fast and accurate algorithm for solving Bernstein-Vandermonde linear systems. Linear Algebra Appl. 422, 616–628.
Moon, H.P., Farouki, R.T., Choi, H.I., 2001. Construction and shape analysis of PH quintic Hermite interpolants. Comput. Aided Geom. Des. 18 (2), 93–115.
Šír, Z., Jüttler, B., 2007. C^2 Hermite interpolation by Pythagorean hodograph space curves. Math. Comput. 76 (259), 1373–1391.